# AN EXPERIMENTAL STUDY ON CYCLIC STRAIN INDUCED CREEP, RELATIONSHIP BETWEEN DIFFERENT MODES OF STRESS AND STRAIN SUPERPOSITION

Y. Nozue*, T. Udoguchi**, Y. Asada** and S. Mitsuhashi**

## INTRODUCTION

The phenomenon of cyclic strain induced creep is observed even at room temperature, when a material is subjected to a cyclic strain and a steady stress. Progressive strain accumulates in the direction of steady stress when cyclic plastic strain is superimposed in any direction. This phenomenon has been studied by several investigators in different loading combinations for various materials [1 - 4]. However, the complete description of the fundamental characteristics of the phenomenon have not been established yet. An important aspect to reveal the mechanism of this phenomenon and to formulate this complex behaviour is to clear up the relationships among plastic strain accumulations due to different modes of superposition of cyclic strain and steady stress.

In the former paper [5], the authors have reported some behaviour of cyclic strain induced creep, i.e., strain accumulation and its recovery. The present paper describes fundamental experiments performed with cylindrical specimens which were subjected to two different modes of stress and strain superposition. The first mode is a combination of the cyclic torsional strain and the steady axial stress (T-A mode), the second is a combination of the cyclic axial strain and the steady torsional stress (A-T mode). On the basis of the experimental data for three kinds of materials (0.45% carbon steel, 6:4 brass and austenitic stainless steel), the authors derived an empirical formula to represent the relationships between the two different modes of stress and strain superposition.

## EXPERIMENTS

The materials used in this investigation were carbon steel JIS-S45C, 6:4 brass and austenitic stainless steel JIS-SUS304. Their chemical compositions and mechanical properties are given in Tables 1 and 2 respectively.

Hollow cylindrical specimens were used and their nominal dimensions are: outside diameter 13～14 mm, inside diameter 10 mm, and gage length 30～50 mm. Actual dimensions of the specimen were a little altered so as to fit the test conditions and strain measuring devices.

A push-pull fatigue tester and a torsional fatigue tester, both controlled by the electro-hydraulic closed-loop system were used together with dead-weight loading mechanism to apply torsional or axial steady stress. Strains were measured and controlled by specially designed electro-mechanical instruments.

* Komatsu Ltd., 2597 Shinomiya, Hiratsuka, Kanagawa, Japan.
** University of Tokyo, 7-3-1 Hongo, Bunkyo, Tokyo, Japan.

The tests were conducted in a low-cycle fatigue region. In A-T mode experiments, cyclic axial strain range $\Delta\varepsilon$ was 1~3%, and in T-A mode experiments, cyclic torsional strain range $\Delta\gamma$ was 2~10%. The wave form of strain cycle was fully reversed triangular, and strain rate $\dot{\varepsilon}$ or $\dot{\gamma}$ was 0.25~1.0%/sec. In all experiments, steady stress ($\tau$ or $\sigma$) was arranged not to exceed 30% of yield stress or 0.2% proof stress (i.e., $|\tau/\tau_y|$ or $|\sigma/\sigma_y| < 0.3$).

Under these conditions, 3~5 levels of cyclic strain and steady stress were selected for each three materials. The total amount of specimens used in the test was more than 100.

## ACCUMULATION OF STRAIN ALONG STEADY STRESS

Typical results of T-A mode experiments are shown in Figures 1 and 2. Each figure shows the case of JIS-S45C and JIS-SUS304 respectively, where the accumulated strain is plotted against the number of strain cycles. It can be seen that similar feature to that of high temperature creep appears here. However, the shapes of these two curves are fairly different. In the case of carbon steel, the slope of the creep curves $d\varepsilon/dN$ continues to decrease until failure, however, for JIS-SUS304 $d\varepsilon/dN$ converges to constant values. This converging behaviour is seen for 6:4 brass, also.

In A-T mode experiments, the same difference of creep curves is observed between carbon steel and 6:4 brass or stainless steel. A remarkable difference between the creep curves at A-T mode and T-A mode is the so-called secondary effect. Namely, in T-A mode, even if no axial stress is applied, the axial strain accumulation caused by secondary effect is observed, whereas in A-T mode, no torsional strain accumulates in the absence of steady torsional stress. Except for this point, creep curve features of A-T mode are quite similar to that of T-A mode. This observation suggests that the relationship between accumulated strains in T-A mode and A-T mode can be formulated by simple equations.

## FORMULATION OF RELATIONSHIP BETWEEN T-A AND A-T MODE

Considering the secondary effect in T-A mode, the strain in the direction of steady stress $\varepsilon$ or $\gamma$ is divided into three components in T-A mode and two components in A-T mode as following:

$$\left.\begin{aligned} &\text{T-A mode} : \varepsilon = \varepsilon_e + \varepsilon_{p\Pi} + \varepsilon_{p\sigma} \\ &\text{A-T mode} : \gamma = \gamma_e + \gamma_{p\tau} \end{aligned}\right\} \quad (1)$$

where $\varepsilon_e$ or $\gamma_e$ is the elastic component by steady stress, i.e., $\varepsilon_e = \sigma/E$ (E is Young's modulus) and $\gamma_e = \tau/G$ (G is Shear Modulus). $\varepsilon_{p\Pi}$ means the secondary axial strain accumulated by torsional strain cycling in T-A mode, so that the component is represented by the following function.

$$\varepsilon_{p\Pi} = \varepsilon_{p\Pi}(\Delta\gamma_p, N) \quad (2)$$

where $\Delta\gamma_p$ is the torsional plastic strain range, and N is the number of its cycles. The relationship between T-A and A-T mode should be discussed





by comparison of $\varepsilon_{p\sigma}$ with $\gamma_{p\tau}$ which are obtained subtracting $\varepsilon_e$ and $\varepsilon_{p\Pi}$ from $\varepsilon$, and $\gamma_e$ from $\gamma$ respectively. The components $\varepsilon_{p\sigma}$ and $\gamma_{p\tau}$ can be represented by the following function.

$$\left.\begin{aligned} &\text{T-A mode} : \varepsilon_{p\sigma} = \varepsilon_{p\sigma}(\sigma/\sigma_y, \Delta\gamma_p, N) \\ &\text{A-T mode} : \gamma_{p\tau} = \gamma_{p\tau}(\tau/\tau_y, \Delta\varepsilon_p, N) \end{aligned}\right\} \quad (3)$$

where $\Delta\varepsilon_p$ is the axial plastic strain range. The formulation of the relationship between $\varepsilon_{p\sigma}$ and $\gamma_{p\tau}$ would be discussed in the following sections.

### Carbon Steel JIS-S45C

By the use of the test results on JIS-S45C specimens, $\varepsilon_{p\sigma}$ and $\gamma_{p\tau}$ can be plotted almost linearly against 2N on log-log scale. An example is shown in Figure 3. Hence, the accumulated strains due to the steady stresses are expressed as

$$\left.\begin{aligned} &\text{T-A mode} : \varepsilon_{p\sigma} = \alpha_\sigma (2N)^{\beta\sigma} \\ &\text{A-T mode} : \gamma_{p\tau} = \alpha_\tau (2N)^{\beta\tau} \end{aligned}\right\} \quad (4)$$

Exponents $\beta_\sigma$ and $\beta_\tau$ obtained from experimental data, can be plotted against $\Delta\gamma_p$ and $2\Delta\varepsilon_p$ respectively as shown in Figure 4. It can be seen from Figure 4 that the exponents are determined only by cyclic strain range, and $\beta_\sigma$ and $\beta_\tau$ are equal when $\Delta\gamma_p = 2\Delta\varepsilon_p$. On the other hand, coefficients $\alpha_\sigma$ and $\alpha_\tau$ are affected by the cyclic strain range and the steady stress, as shown in Figure 5. However, a similar relation to that in the exponents $\beta_\sigma$ and $\beta_\tau$ exists here. Namely, if $\Delta\gamma_p = 2\Delta\varepsilon_p$ and $\sigma/\sigma_y = \tau/\tau_y$, coefficients $\alpha_\sigma$ and $\alpha_\tau$ take an equal value.

Finally, $\alpha_\sigma$, $\alpha_\tau$, $\beta_\sigma$ and $\beta_\tau$ can be expressed as follows:

$$\left.\begin{aligned} &\alpha_\sigma = k_1 \cdot (\sigma/\sigma_y)^{k_2} (\Delta\gamma_p)^{k_3} \\ &\alpha_\tau = 2 \cdot k_1 \cdot (\tau/\tau_y)^{k_2} (2\Delta\varepsilon_p)^{k_3} \\ &\beta_\sigma = f(\Delta\gamma_p), \quad \beta_\tau = f(2\Delta\varepsilon_p) \end{aligned}\right\} \quad (5)$$

where $k_1$, $k_2$ and $k_3$ are the material constants and probably temperature dependent. In the case of JIS-S45C at room temperature, $k_1 = 1.5$, $k_2 = 1.1$ and $k_3 = 0.9$.

### 6:4 Brass and Stainless Steel JIS-SUS304

The experimental data of 6:4 brass and JIS-SUS304 cannot be plotted linearly on log-log scale as in the case of JIS-S45C, however $\varepsilon_{p\sigma}$ and $\gamma_{p\tau}$ can be expressed by the following empirical formulas in the present cases.

$$\left.\begin{aligned} &\text{T-A mode} : \varepsilon_{p\sigma} = C_\sigma(\sigma/\sigma_y)\cdot F_\sigma(\Delta\gamma_p\ ,\ N) \\ &\text{A-T mode} : \gamma_{p\tau} = C_\tau(\tau/\tau_y)\cdot F_\tau(\Delta\varepsilon_p\ ,\ N) \end{aligned}\right\} \quad (6)$$

Figure 6 shows that the relations of $C_\sigma$ vs. $\sigma/\sigma_y$ and $C_\tau$ vs. $\tau/\tau_y$ obtained from the experiments of 6:4 brass coincide with each other fairly well. Moreover, as shown in Figure 7, $2F_\sigma$ and $F_\tau$ plotted against N are almost equal when the parameters $\Delta\varepsilon_p$ and $\Delta\gamma_p/2$ are taken equal. Hence,

$$\left.\begin{aligned} &C_\tau(x) = C_\sigma(x) \\ &F_\tau(y/2\ ,\ N) = 2\cdot F_\sigma(y\ ,\ N) \end{aligned}\right\} \quad (7)$$

Finally, in the present case of 6:4 brass, accumulated strains due to the steady stress, $\varepsilon_{p\sigma}$ and $\gamma_{p\tau}$, can be expressed as follows:

$$\left.\begin{aligned} &\text{T-A mode} : \varepsilon_{p\sigma} = C(\sigma/\sigma_y)\cdot F(\Delta\gamma_p\ ,\ N) \\ &\text{A-T mode} : \gamma_{p\tau} = 2\cdot C(\tau/\tau_y)\cdot F(2\Delta\varepsilon_p\ ,\ N) \end{aligned}\right\} \quad (8)$$

Almost the same formulation as with the case of 6:4 brass can be applied to the case of JIS-SUS304. However, the coincidence of $C_\tau$ and $C_\sigma$, or $F_\tau$ and $F_\sigma$ is not so good as compared with the case of 6:4 brass, and the coefficients take different values. The final results for JIS-SUS304 corresponding to Equation (8) are:

$$\left.\begin{aligned} &\text{T-A mode} : \varepsilon_{p\sigma} = C(\sigma/\sigma_y)\cdot F(\Delta\gamma_p\ ,\ N) \\ &\text{A-T mode} : \gamma_{p\tau} = 0.75\cdot C(\tau/\tau_y)\cdot F(3.4\Delta\varepsilon_p\ ,\ N) \end{aligned}\right\} \quad (9)$$

## CONCLUSIONS

The present paper presents an empirical relationship between the two modes of cyclic strain induced creep due to the different stress and strain superposition, i.e., the combination of cyclic torsional strain and steady axial stress (T-A mode), and the combination of cyclic axial strain and steady torsional stress (A-T mode). On the basis of the test results obtained by experiments with specimens of more than 100, the following generalized relationship was obtained empirically:

$$\left.\begin{aligned} &\text{T-A mode} : \varepsilon_{p\sigma} = f(\sigma/\sigma_y\ ,\ \Delta\gamma_p\ ,\ N) \\ &\text{A-T mode} : \gamma_{p\tau} = c_1\cdot f(\tau/\tau_y\ ,\ c_2\Delta\varepsilon_p\ ,\ N) \end{aligned}\right\} \quad (10)$$

where $c_1 = c_2 = 2.0$ for carbon steel JIS-S45C and 6:4 brass. This relationship can be called "Tresca Type Equivalence". However, this equivalence cannot be applied to the case of austenitic stainless steel JIS-SUS304, where $c_1 = 0.75$ and $c_2 = 3.4$.






## REFERENCES

1. COFFIN, L. F., Jr., Trans. ASME Ser. D, 82, 1960, 671.
2. BENDLER, H. M. and WOOD, W. A., Trans. AIME, 224, 1962, 18.
3. MOYAR, G. J. and SINCLAIR, G. M., Joint International Conference on Creep, 2, 1963, 47.
4. RONAY, M., ASTM STP 404, 1966, 176.
5. UDOGUCHI, T. and ASADA, Y., International Conference on Creep and Fatigue in Elevated Temperature Applications, Philadelphia, Pennsylvania, 1975, Paper C210/73.


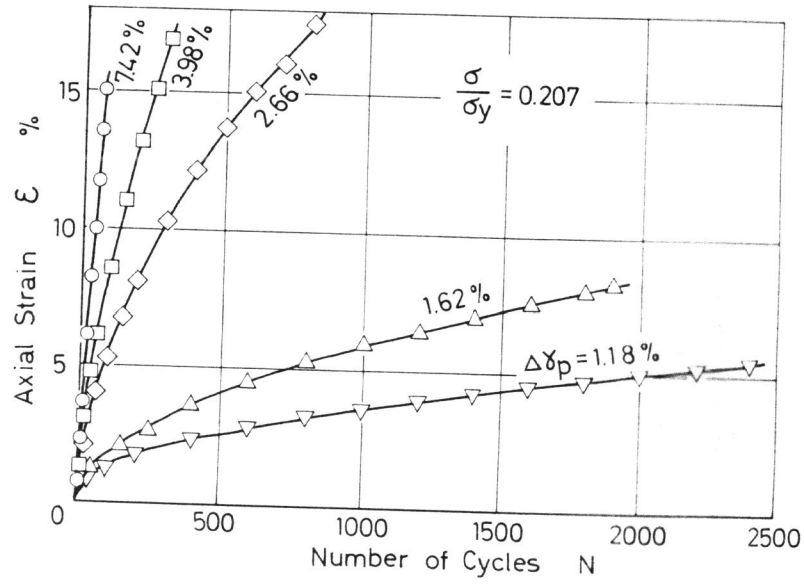


Figure 1 Strain Accumulation Along Steady Axial Stress When Torsional Strain is Cycled. Material: JIS-S45C Carbon Steel

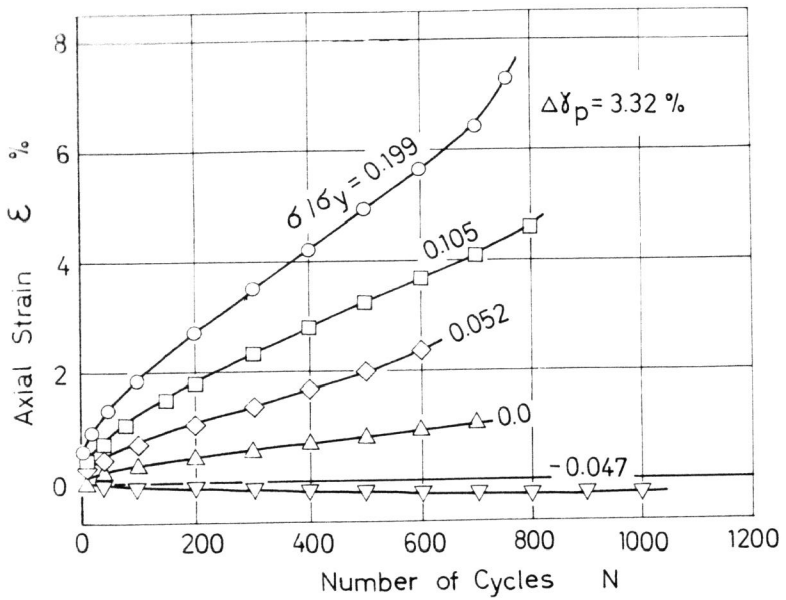


Figure 2 Strain Accumulation Along Steady Axial Stress when Torsional Strain is Cycled. Material: JIS-SUS304 Stainless Steel

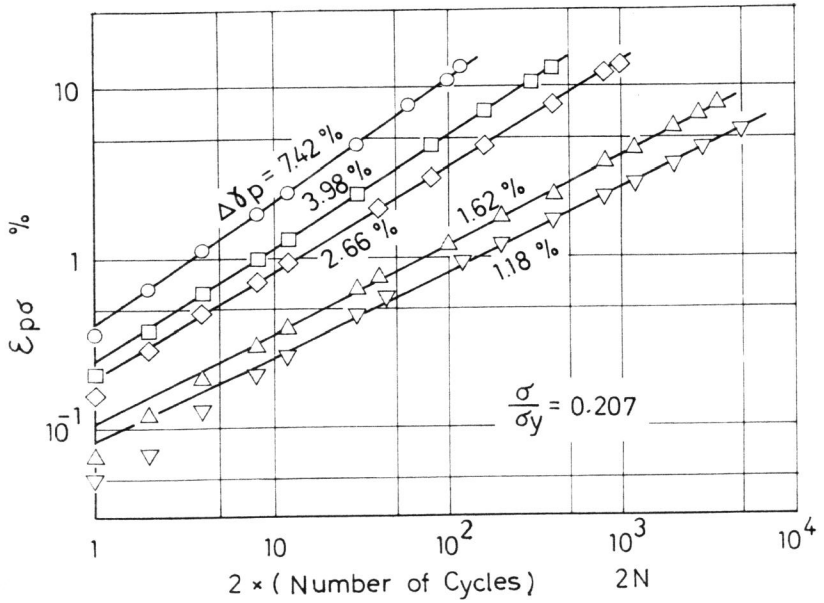


Figure 3 Linear Relationship on Log-Log Scale Between Accumulated Strain $\varepsilon_{p\sigma}$, and Number of Strain Cycles N. Material: JIS-S45C





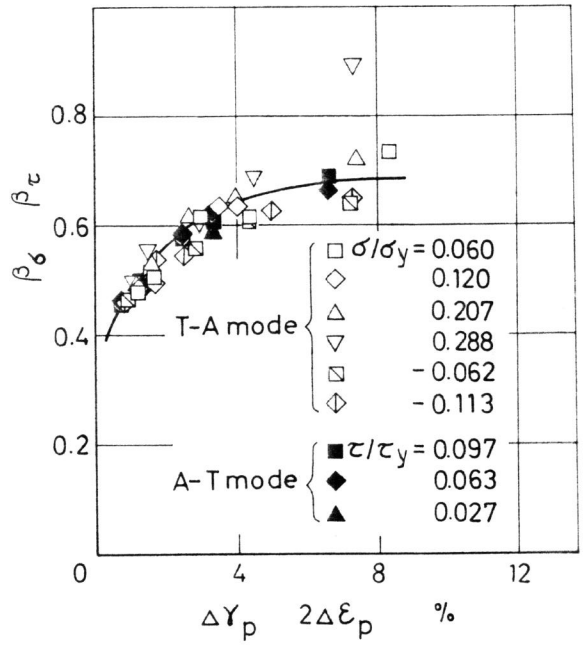


Figure 4 Comparison of Exponent $\beta_\sigma$ with $\beta_\tau$, where $\beta_\sigma = \beta_\sigma(\Delta\gamma_p)$ and $\beta_\tau = \beta_\tau(\Delta\varepsilon_p)$. Material: JIS-S45C

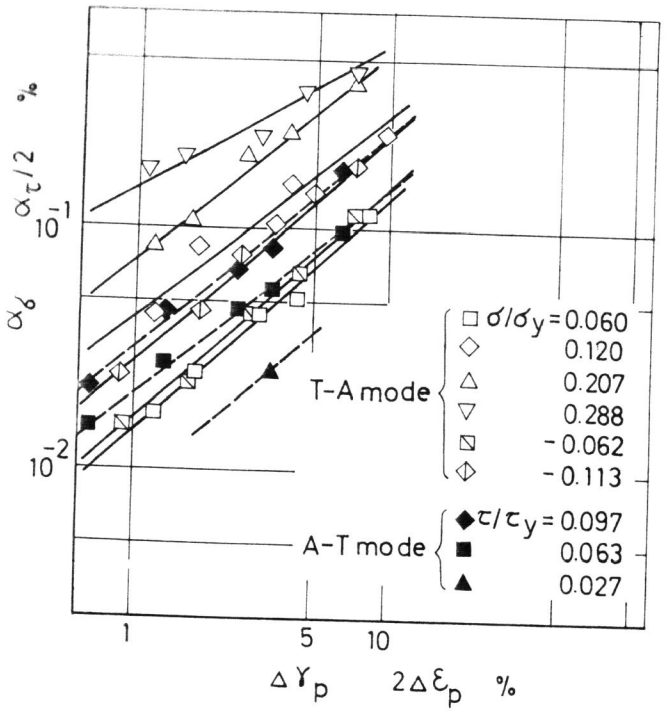


Figure 5 Comparison of Coefficient $\alpha_\sigma$ with $\alpha_\tau$, where $\alpha_\sigma = \alpha_\sigma(\sigma/\sigma_y, \Delta\gamma_p)$ and $\alpha_\tau = \alpha_\tau(\tau/\tau_y, \Delta\varepsilon_p)$. Material: JIS-S45C

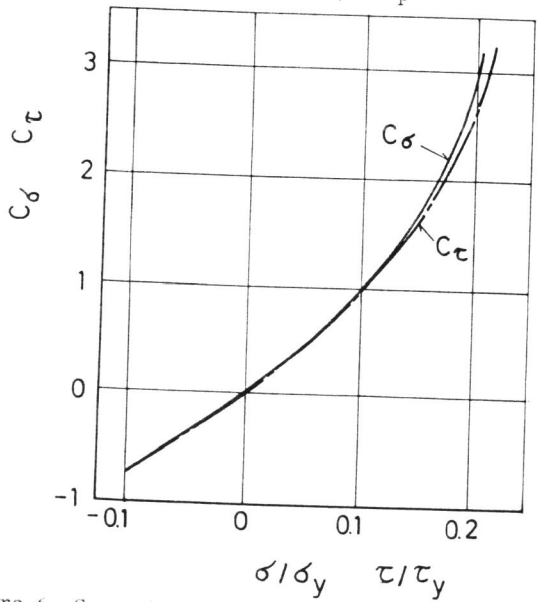


Figure 6 Comparison of $C_\sigma$ with $C_\tau$, where $C_\sigma = C_\sigma(\sigma/\sigma_y)$ and $C_\tau = C_\tau(\tau/\tau_y)$. Material: 6:4 Brass





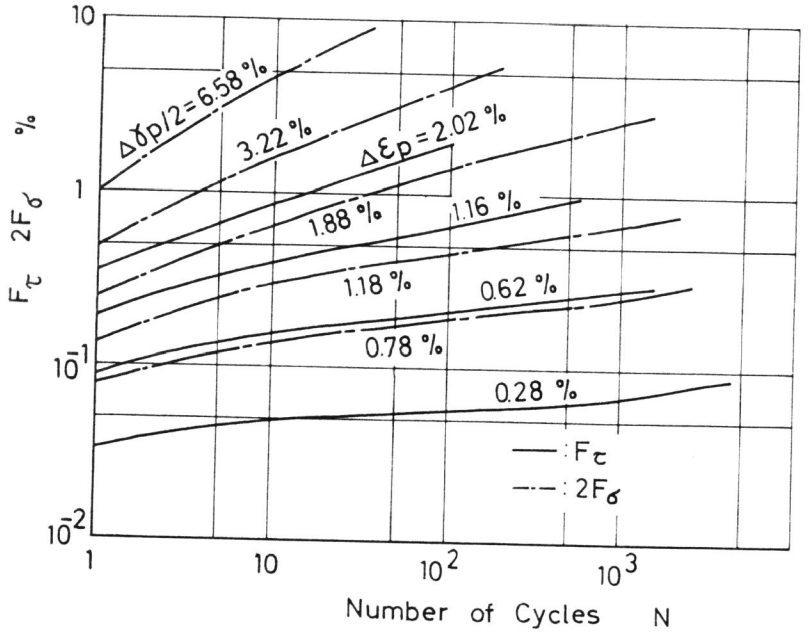


Figure 7 Comparison of $F_\sigma$ with $F_\tau$, where $F_\sigma = F_\sigma(\Delta\gamma_p, N)$ and $F_\tau = F_\tau(\Delta\varepsilon_p, N)$. Material: 6:4 Brass

Table 1 Chemical Compositions of Materials Tested

| | | | | | | | | |
|---|---|---|---|---|---|---|---|---|
| JIS-S45C | C | Si | Mn | P | S | Ni | Cr | Mo |
| | 0.45 | 0.29 | 0.92 | 0.016 | 0.005 | 0.05 | 0.05 | 0.01 |
| JIS-SUS304 | C | Si | Mn | P | S | Ni | Cr | Cu |
| | 0.06 | 0.58 | 1.65 | 0.02 | 0.006 | 9.40 | 18.6 | 0.03 |
| 6:4 Brass | Cu | Pb | Fe | Zn | | | | |
| | 60.0 | 0.01 | 0.02 | Rem. | | | | |

Unit: %

Table 2 Mechanical Properties of Materials Tested

| | Yield Stress or 0.2 % Proof Stress in Tension | Yield Stress or 0.2 % Proof Stress in Shear | U.T.S. | Reduction in Area |
|---|---|---|---|---|
| JIS-S45C | 485 MPa | 315 MPa | 779 MPa | 68.5 % |
| JIS-SUS304 | 237 MPa | 145 MPa | 622 MPa | 82.0 % |
| 6:4 Brass | 299 MPa | 180 MPa | 439 MPa | 34.2 % |